Cytoplasmic RNA in Nervous System Tumours in Children: A Fluorochromic Histochemical Study using Acridine Orange

Harvey B. Sarnat, Bernadette Curry, N.B. Rewcastle and Cynthia L. Trevenen

ABSTRACT: Acridine orange was used as a fluorochromic histochemical stain of nucleic acids, applied to 78 neoplasms of the central and peripheral nervous systems of 60 children. Some cases were compared with 5 adults and 4 other cases of chronic reactive gemistocytic gliosis. Opposite concentration gradients of cytoplasmic ribonucleic acid (RNA) was demonstrated in tumours of the neuronal/neuroectodermal series, and those of the glial/neuroepithelial series. Minimal AO-RNA fluorescence was seen in 8 cerebellar medulloblastomas and in a retinoblastoma; strong AO-RNA fluorescence occurred in one cerebellar medulloblastoma and in 3 primitive neuroectodemal tumours of the cerebral cortex. Intermediate intensity of fluorescence was found in neuroblastomas, and strong fluorescence was shown in well differentiated ganglioneuroma cells and in cells of chromaffin tumours. Among glial tumours, by contrast, the most anaplastic cells displayed the most RNA fluorescence, while better differentiated astrocytoma cells showed much less. Gradients also were found within some astrocytomas, corresponding to zones of relative anaplasia. Minimal or no fluorescence was detected in reactive gemistocytes or in oligodendroglioma cells. Ependymomas were weakly fluorescent and choroid plexus papillomas showed more fluorescence, similar to the findings in normal ependyma and choroid plexus. Several non-neuroepithelial tumours of the nervous system and Schwannomas also were studied. The acridine orange technique applied to either frozen or paraffin sections of nervous system tumours, has value as an adjunct in the diagnosis and grading of these neoplasms and perhaps in distinguishing reactive gliosis from benign astrocytoma.

RÉSUMÉ: L'A.R.N. dans les tumeurs du système nerveux chez des enfants en employant l'acridine-orange comme un colorant fluorochromique histochimique Nous avons employé l'acridine-orange comme colorant fluorochromique histochimique, en étudiant 78 néoplasmes des systèmes nerveux central et périphérique chez 60 enfants. Quelques cas furent comparés aux tumeurs de 5 adultes et aussi avec 4 autres cas de gliose réactive gémistocytaire. On a trouvé que les gradients à concentration d'ARN cytoplasmique dans la série neuronale/neuroectodermique et dans la série gliale/neuroépithéliale étaient différents. On montra un minimum de fluorescence d'AO-ARN dans 8 médulloblastomes cérébelleux et dans un rétinoblastome. L'intensité de la fluorescence trouvée dans les neuroblastomes était intermédiaire, et une fluorescence forte fut montrée dans les cellules des ganglioneuromes bien différenciés et des tumeurs chromaffines. Cependant une telle fluorescence forte était également évidente dans un médulloblastome et dans 3 tumeurs neuroectodermiques primitives du cortex cérébral. Par contraste, chez les tumeurs gliales les cellules les plus anaplastiques étaient celles qui montraient la fluorescence d'ARN la plus forte, tandis que les cellules d'astrocytomes mieux différenciées en avaient le moins. On trouva aussi des gradients dans quelques astrocytomes, qui correspondaient aux zones d'anaplasie relative. On aperçu très peu ou aucune fluorescence d'ARN dans les gémistocytes réactifs ou dans les cellules d'oligodendrogliome. Les épendymomes montrèrent une fluorescence faible et les papillomes du plexus choroïde montrèrent plus de fluorescence d'ARN, semblable à celle des structures normales. On étudia également plusieurs autres tumeurs non neuroépithéliales du système nerveux. La technique d'acridine-orange, appliquée à des coupes de tumeurs du système nerveux, soit congélées soit en paraffine, offre un avantage comme colorant supplémentaire pour le diagnostic et le degré de ces néoplasmes et aussi peut être utile pour distinguer la gliose réactive de l'astrocytome bénin.

Can. J. Neurol. Sci. 1986; 13:31-41

From the Departments of Pathology, Paediatrics, and Clinical Neurosciences, University of Calgary Faculty of Medicine, Calgary, Alberta

Portions of this study were presented at the XIX Canadian Congress of Neurological Sciences, Edmonton, Alberta, June 27-30, 1984, and at the Child Neurology Society annual meeting, Memphis, Tennessee, USA, October 10-12, 1985

Received April 18, 1985. Accepted in revised form November 14, 1985

Reprint requests to: Dr. H.B. Sarnat, Alberta Children's Hospital, 1820 Richmond Road S.W., Calgary, Alberta, Canada T2T 5C7

Acridine orange (AO) is a fluorochromic stain of nucleic acids which has been applied to muscle biopsies to identify regenerating or denervated myofibres by their relatively increased concentration of sarcoplasmic ribonucleic acid (RNA).[1,2] Neurons and other secretory cells have the highest cytoplasmic RNA content of any cells of the body under physiological conditions; the brilliant orange AO fluorescence of neurons in the central nervous system contrasts sharply with the pale green background of glial cells and neuropil.[2] In the peripheral nervous system AO vividly demonstrates small ganglion cells in the myenteric plexus of the terminal colon in young infants, locating neurons that are often difficult to identify histologically in suspected cases of Hirschsprung's disease.[2,3]

The application of histochemical and immunocytochemical techniques to sections of brain tumours can assist in their diagnosis, classification, and grading. In this study we applied AO to sections of a variety of nervous system neoplasms in children. A few adults were included for comparative purposes in some cases. Differences found among the several types and grades of tumours suggest that the relative cytoplasmic RNA content of neoplastic cells, as demonstrated by AO fluorochrome, may provide a new supplementary criterion for the diagnosis of neoplasms in the nervous system.

Materials and Methods

Tumours resected from the central and peripheral nervous systems or found at autopsy between January 1980 and July 1985 were identified from records of the Departments of Pathology at Alberta Children's Provincial Hospital and Foothills Regional Provincial Hospital in Calgary. A total of 78 specimens were examined from 65 patients (60 children and 5 adults), some specimens being repeat biopsies of recurrent tumours in the same patients. The ages of the children ranged from the neonatal period to late adolescence. Five adults were included because their tumours were not available among the pediatric cases and were thought to be important for comparison, or were included for comparison with single childhood examples of these tumours. Approximately 72 percent of the tumours (56/78) were in the central nervous system, the others arising peripherally.

Based on histological findings, tumours were classified into three categories (Table 1): 1) neuronal/neuroectodermal series (medulloblastoma; retinoblastoma; primitive neuroectodermal tumour; neuroblastoma; ganglioneuroma; ganglioglioma; pheochromocytoma; carotid body tumour); 2) glial/neuroepithelial series (astrocytomas of all grades; oligendroglioma; choroid plexus papilloma; ependymoma; neuroectodermal or colloid cyst); 3) other miscellaneous lesions not of neuronal or glial origin but within the nervous system (craniopharyngioma; pineal germinoma; epidermoid; dermoid; chordoma; Schwannoma; metastatic Ewing sarcoma in brain). Pituitary neoplasms, meningiomas, and neurofibromas were not included in this study because none were resected from children in our institutions during the study period.

Sections of brain exhibiting reactive astrocytosis including gemistocytes also were examined with AO by the same technique in four other patients, for comparison with astrocytic tumours. Normal brain tissue, dorsal root and autonomic ganglia including the myenteric plexus of the terminal colon, and adrenal medulla from several patients of all ages were available for comparison.

Histological slides were reviewed and representative sections were selected. Additional paraffin-embedded sections were then cut from the remaining tissue blocks. In 1985, 1984, and the second half of 1983, during the course of the study, cryostat sections of unfixed frozen tissue also were prepared from most of the new cases; formalin-fixed, paraffin-embedded sections of these same tumours were also examined in each case.

Sections of the tumours were stained with acridine orange (AO) according to methods previously described.[2] They were immediately examined in a Leitz epifluorescence ultraviolet microscope, using a BG-12 transmission filter. Photographs were taken using Kodak ET-135 film for tungsten light (ASA 160) for diapositive transparencies, the exposure time generally being 5 to 20 seconds.

After examination of the sections under ultraviolet light, the coverslips were removed from the wet mounts and the sections rinsed with 0.067 M phosphate buffer at pH 6.0. The sections then were processed for staining with hematoxylin-eosin and permanently mounted.

In all categories of tumours, representative cases were reexamined after ribonuclease digestion. After AO staining and examination in the fluorescence microscope, these sections were rinsed and then incubated for one hour with bovine pancreatic ribonuclease; the sections were then restained with AO, examined under ultraviolet light, and rephotographed. This supplementary procedure was then followed by another rinse in phosphate buffer and staining with hematoxylin-eosin.

The intensity of cytoplasmic RNA fluorescence was qualitatively graded on a scale of 0 to ++++, representing no orange fluorescence to maximal intensity. Scoring was recorded

Table 1: Types of tumours examined with acridine orange technique

Neuronal/Neuroectodermal Series		
medulloblastoma	9	
retinoblastoma	1	
primitive neuroectodermal tumour	4	
neuroblastoma	5	
ganglioneuroma	7	
ganglioglioma	1	
pheochromocytoma	2	
carotid body tumour	1	TOTAL 29 biopsies
Neuroglial/Neuroepithelial Series		
astrocytoma, benign	17	
astrocytoma, malignant	11	
oligodendroglioma	2	
ependymoma	2	
choroid plexus papilloma	2	
neuroepithelial cyst	1	TOTAL 35 biopsies
Non-Neuronal/Glial Tumour Series		
pineal germinoma	1	
craniopharyngioma	2	
lipoma	1	
epidermoid	1	
dermoid	1	
chordoma	2	
Ewing sarcoma, metastatic to brain	1	
Schwannoma	3	TOTAL 12 biopsies

https://doi.org/10.1017/S0317167100035769 Published online by Cambridge University Press

twice, first at the time of examination in the fluorescence microscope, and again from the photomicrographic transparencies made of each case, but no discrepency was found.

The quality of staining was equally good in unfixed frozen and formalin-fixed, paraffin-embedded sections in cases in which both types of sections were available. In a few cases where formalin fixation had been prolonged or the tissue had been stored for a year or more, a diffuse artifactual staining was seen, the entire section appearing uniformly orange. Exposure of small microscopic fields to ultraviolet light for five or six minutes extinguished this artifactual diffuse orange colour before quenching the physiological fluorescence of RNA which occurred only after 10 to 15 minutes, as previously demonstrated.[2]

Results

Tables 2 to 4 are the three designated categories of neoplasms in this study, and summarize the data from all patients. Consistency was seen among different tumours of the same type and grade from different patients. One of the most striking findings was the gradient of intensity of orange AO-RNA fluorescence observed among tumour cells of different morphological maturity or pleomorphism. Some astrocytomas also exhibited internal gradients similar to the variable degrees of histological anaplasia within these tumours.

Tumours of the Neuronal/Neuroectodermal Series (Table 2; Figures 1-7)

Cells in 8 of the 9 cerebellar medulloblastomas (Figure 1) and the retinoblastoma showed very little orange colour in their cytoplasm, the non-neoplastic cells of the fibrovascular septae often displaying more orange fluorescence than the tumour cells. Neuroblastoma cells (Figure 4) showed more cytoplasmic RNA fluorescence than medulloblastoma cells, but not nearly as much as the mature neuronal tumour cells of the ganglioneuromas (Figures 5, 6) ganglioglioma, or chromaffin cell tumours: pheochromocytoma (Figure 7) and carotid body tumour. The most mature neoplastic neuronal cells resembled normal neurons in the amount of brilliant granular orange-red colour of their cytoplasm. In ganglioneuroblastomas consisting of a mixture of immature and maturing neuronal cell types, the amount of AO-RNA fluorescence in the cytoplasm varied according to the morphological maturity of the individual cell. However, the intensity of fluorescence was not simply a function of the amount of cytoplasm of each cell. For example, the cytoplasmic extensions of medulloblastoma cells toward the center of rosettes were not more orange than the thin rim of perinuclear cytoplasm. Whether the tumour arose in the central or the peripheral nervous system was not a determinant factor in the quality or intensity of AO-RNA fluorescence.

Only one of the 9 cerebellar medulloblastomas showed strong AO-RNA fluorescence (Figure 2), but primitive neuroectodermal tumours arising in the cerebral cortex exhibited highly luminescent orange cytoplasm (Figure 3). This colour disappeared after incubation with ribonuclease. Immunocytochemical stains for glial fibrillary acidic protein (GFAP), S-100 protein, and alpha-fetoprotein were negative in these tumours, despite the resemblance with AO stain to the malignant astrocytomas. Electron microscopy confirmed an abundance of free ribosomes and rough endoplasmic reticulum and microtubular differentiation in the cytoplasm of these strongly AO-RNA positive cells from one medulloblastoma (Figure 19) as well as from the supratentorial primitive neuroectodermal tumours. The remainder of the cerebellar medulloblastomas had few ribosomes seen ultrastructurally.

Tumours of the Neuroglial/Neuroepithelial Series (Table 3; Figures 8-15)

In the glial line, a gradient also was found to be related to maturity or degree of pleomorphism, but this gradient was the opposite of that seen in neuronal neoplasms. Well differentiated low grade astrocytoma cells and the clear cells of oligodendrogliomas had very little cytoplasmic RNA demonstrated by AO (Figures 9, 10). Non-neoplastic chronic reactive astrocytes including gemistocytes showed almost none (Figure 8). By contrast, the more anaplastic tumours with highly pleomorphic malignant astrocytes had abundant AO-RNA fluorescence (Figures 11, 12). The degree of orange cytoplasmic colour was unrelated to the relative amount of cell cytoplasm. Rosenthal fibres remained green (Figure 13), as with other tissue containing no nucleic acids.

The gradient described for the glial cell line was observed not only between different tumours of varying grade, but also within a single tumour or even in the same section, in cases where the cells were not uniform, but showed varying degrees of maturation or direction of differentiation in different portions of these mixed tumours. Areas of mixed gliomas histologically differentiated into mainly oligodendrocytes showed AO-RNA staining characteristics of oligodendroglioma.

Ribonuclease digestion completely abolished the orange colour of astrocytoma cells, both benign and malignant.

Cuboidal epithelial cells of choroid plexus papillomas showed moderately strong cytoplasmic orange fluorescence (Figure 14), but this quality was nearly identical to that seen in normal choroid plexus of both young infants and adults. Well differentiated ependymomas showed mild AO-RNA fluorescence (Figure 15), the same or slightly more than seen in normal ependyma. Cells forming rosettes and pseudorosettes did not display more orange cytoplasmic fluorescence than did other ependymal cells.

Non-Neuroectodermal Tumours of the CNS (Table 4; Figures 16-18)

The large spheroidal epithelioid cells of a pineal germinoma showed strong cytoplasmic AO-RNA fluorescence, but the small lymphocytic cells in this tumour had only moderate fluorescence (Figure 16).

Craniopharyngiomas showed no AO-RNA fluorescence, as expected (Figure 17). A lipoma also was negative. An epidermoid and a dermoid were weakly fluorescent. Chordoma cells were strongly fluoresecent for RNA (Figure 18), correlating well with the ultrastructural appearance (Figure 20). The three Schwannomas were all quite similar, showing a moderate degree of orange colour in their cytoplasm which disappeared completely after ribonuclease digestion.

Cells of a metastatic Ewing sarcoma in the brain were positive for AO-RNA fluorescence. Other sarcomas not involving the nervous system also were examined for comparison. These tumours included a synovial sarcoma of the knee and a rhabdomyosarcoma of the pelvis in children and showed similar strong orange cytoplasmic fluorescence.

Connective Tissue RNA

Connective tissue components of some tumours often showed

Table 2: Tumours of the Neuronal/Neuroectodermal Series (29 biopsies)

Patient	Age/Sex	Site	Pathological Diagnosis	Cytoplasmic AO-RNA Fluorescence
1	21 mo/M	cerebellum	medulloblastoma	±
2	20 mo/F	cerebellum	medulloblastoma	+
3	12 mo/F	cerebellum	medulloblastoma	+
4	14 mo/M	cerebellum	medulloblastoma	+
5	13 yr/M	cerebellum	medulloblastoma; astrocytoma component	+
6	9 yr/M	cerebellum	medulloblastoma; oligodendroglioma component	+
7	3 yr/M	cerebellum	medulloblastoma; astrocytoma component	+ +
8	4 yr/F	cerebellum	medulloblastoma	+ +
9	5 yr/M	eye	retinoblastoma	±
10	15 mo/M	cerebellum	medulloblastoma/primitive neuroectodermal tumour with microtubular differentiation; astrocytoma component	+ + +
11	4 yr/M	frontal	primitive neuroectodermal tumour	+ + + +
12A	6 yr/M	parieto-occipital	primitive neuroectodermal tumour	+ + + +
12B	7 yr/M	parieto-occipital	primitive neuroectodermal tumour	+ + + +
13	9 mo/M	presacral	neuroblastoma	+ +
14	2 yr/M	retroperitoneal	neuroblastoma	+ +
15	21 mo/F	lymph node; pancreas	neuroblastoma	+ + +
16A	7 wk/M	retroperitoneal; lymph node	neuroblastoma	+ + +
16B	3 mo/M	liver	neuroblastoma/ganglioneuroma	+ + +
17A	3 yr/F	adrenal medulla; para-aortic lymph nodes	neuroblastoma	+ +
17B	4 yr/F	retroperitoneal	ganglioneuroma	+ + + +
17C	8 yr/F	retroperitoneal	ganglioneuroma	+ + + +
18A	19 mo/F	spinal epidural	ganglioneuroma	+ + + +
18B	2 yr/F	retroperitoneal; intervertebral foramen	ganglioneuroma	+ + + +
19	3 yr/M	posterior mediastinum	ganglioneuroma	+ + + +
20	3 mo/M	thoracic sympathetic chain	ganglioneuroma	+ + + +
21	16 yr/M	deep parietal, subcortical	ganglioglioma	+ + + +
22A	14 yr/M	adrenal medulla	pheochromocytoma	+ + + +
22B	15 yr/M	adrenal medulla; retroperitoneal	pheochromocytoma	+ + + +
23	53 yr/F	common carotid bifurcation	carotid body tumour	+ + + +

Key to Tables 2-4: wk = week; mo = month; yr = year; F = female; M = male
Letters after patient number indicate repeat biopsy of same patient for recurrence of tumour
Intensity of orange-red cytoplasmic fluorescence: O = none; ± = slight; + = weak; + + = moderate; + + + = strong; + + + + = very intense.

strong fluorescence. The septal fibroblasts and pericytes of some medulloblastomas have already been mentioned. In recurrent tumours that had received radiation therapy, proliferating fibroblasts had intensely orange fluorescence which disappeared after incubation in ribonuclease.

Cytological Detail of the AO Fluorescence

Mature normal neurons in general show strong AO fluorescence for cytoplasmic RNA. In motor neurons, the orange colour is seen as coarsely granular, closely packed material corresponding to the parallel arrays of rough endoplasmic reticulum that comprise the Nissl substance.[2] Dorsal root ganglion cells, primary somatosensory neurons, have a similar appearance with AO stain. In most other neurons the orange colour is more dispersed in the cytoplasm as finely granular material or have a diffusely orange ground glass appearance.

In the better differentiated neoplastic neurons, as in the ganglioneuroma or pheochromocytoma, the orange cytoplasmic fluorescence usually appeared as either finely or coarsely granular material (Figures 5-7), reminiscent of normal mature neurons.

PLATE I (Figs 1-6)

Figure 1 — Patient 6. Densely cellular medulloblastoma of cerebellum in a 9-year-old boy. Only minimal orange colouration is seen in the cytoplasm. AO X400

Figure 2 — Patient 10. The cerebellar medulloblastoma in this 15-month-old boy differed from the other 8 in this series because of the abundant cytoplasmic RNA, confirmed by electron microscopy (Fig 19). AO X250

Figure 3 — Patient 11. Primitive neuroectodermal tumour from cerebral cortex of frontal lobe of a 4-year-old boy, showing strong AO-RNA fluorescence. AO X250

Figure 4 — Patient 13. Neuroblastoma of presacral region in a 9-month-old boy. Neoplastic nerve cells show moderate cytoplasmic fluorescence, but not as much as in mature neurons. AO X250

Figure 5 — Patient 17. Ganglioneuroma of retroperitoneal space in an 8-year-old girl. Well differentiated nerve cells show intensely fluoresecent AO-RNA complexes. AO X400

Figure 6 — Patient 18. Retroperitoneal ganglioneuroma in a 2-year-old girl. Strong orange granular cytoplasmic fluorescence is similar to that seen in normal neurons. AO X400

https://doi.org/10.1017/S0317167100035769 Published online by Cambridge University Press

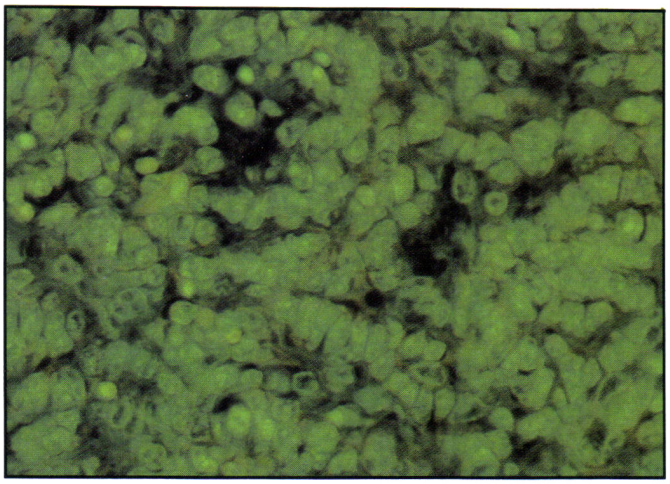

1

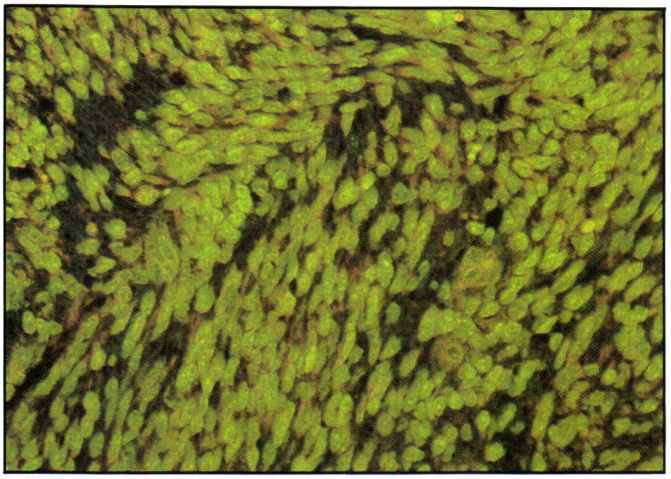

2

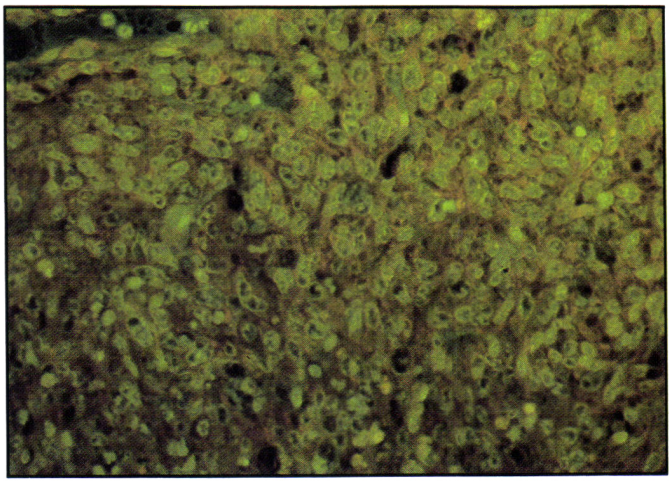

3

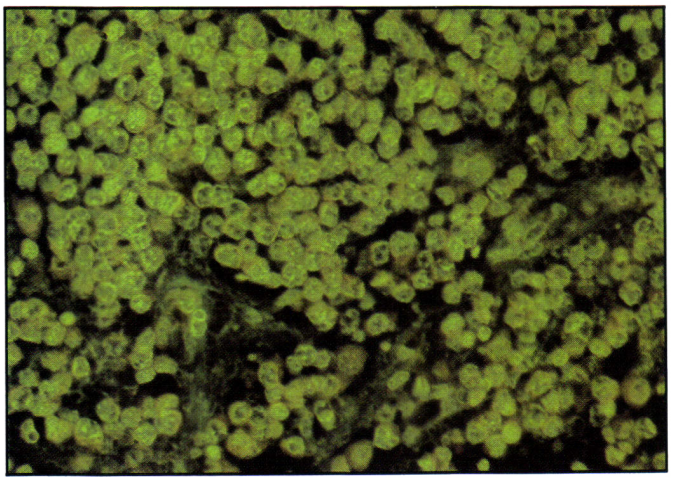

4

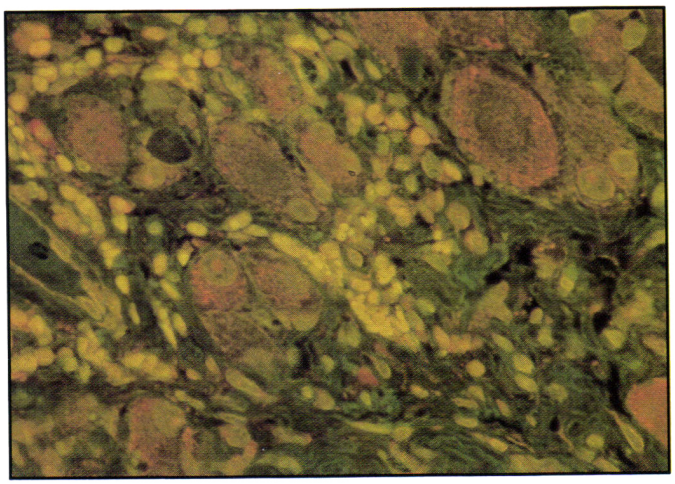

5

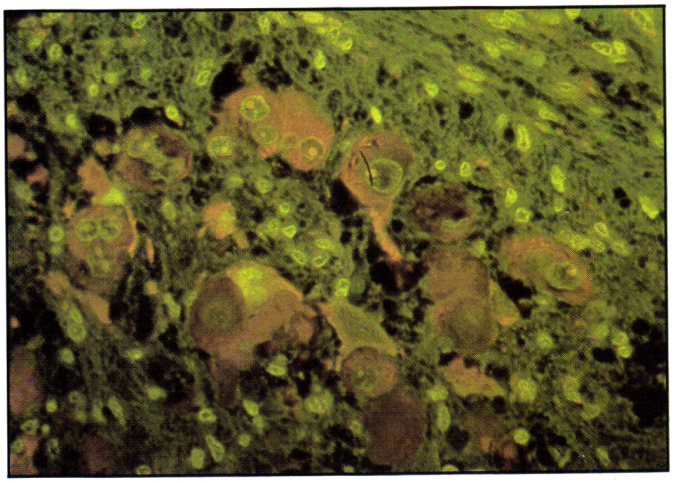

6

https://doi.org/10.1017/S0317167100035769 Published online by Cambridge University Press

Table 3: Tumours of the Neuroglial/Neuroepithelial Series (35 biopsies)

Patient	Age/Sex	Site	Pathological Diagnosis	Cytoplasmic AO-RNA Fluorescence
24	15 yr/F	spinal cord	astrocytoma, well differentiated	+ +
25	5 yr/F	cerebellum	astrocytoma, well differentiated	+
26	7 yr/M	cerebellum	astrocytoma, cystic, well differentiated	+ +
27A	4 yr/F	cerebellum	astrocytoma, well differentiated	+
27B	6 yr/F	cerebellum	astrocytoma, well differentiated	+
28	7 yr/F	thalamus	astrocytoma, pilocytic	+
29	10 yr/F	cerebellum	astrocytoma, well differentiated	+ +
30A	15 yr/F	cerebellum	astrocytoma, well differentiated	+ +
30B	17 yr/F	cerebellum	astrocytoma, well differentiated; calcifications and many Rosenthal fibres	+ +
31	8 yr/M	cerebellum	astrocytoma, cystic, fibrillary	+ +
32A	12 mo/F	cervical spinal cord	astrocytoma, well differentiated	+ +
32B	2 yr/M	cervical spinal cord	astrocytoma, well differentiated, fibrillary	+ +
33	3 yr/M	cerebellum	astrocytoma, fibrillary	+ +
34	9 yr/F	cerebellum	astrocytoma, well differentiated, microcystic	+ +
35	11 yr/M	optic chiasm	astrocytoma, pilocytic	+ +
36	12 yr/M	temporal	astrocytoma, differentiated; cortical infiltration	+ +
37A	3 mo/M	fronto-temporal	astrocytoma, well differentiated	+ +
37B	22 mo/M	fronto-temporal	astrocytoma, malignant	+ + +
38	7 yr/F	cerebellum	astrocytoma, malignant	+ + +
39	10 yr/M	thalamus	astrocytoma, malignant	+ + +
40	8 yr/M	brainstem	astrocytoma, malignant	+ + +
41	12 yr/F	brainstem	astrocytoma, malignant	+ + + +
42	5 mo/F	frontal	astrocytoma, malignant	+ + +
43A	3 yr/F	fronto-temporo-parietal	astrocytoma, malignant	+ + +
43B	3 yr/F	fronto-temporo-parietal	astrocytoma, malignant	+ + + +
43C	3 yr/F	fronto-temporo-parietal	astrocytoma, malignant	+ + + +
44	15 yr/F	parieto-occipital	xanthoastrocytoma, malignant	+ + +
45	9 yr/M	frontal	oligodendroglioma/astrocytoma, well differentiated	+
46A	3 yr/M	temporo-parietal	astrocytoma, fibrillary; many Rosenthal fibres	+
46B	6 yr/M	temporo-parietal	oligodendroglioma/astrocytoma, well differentiated	+
47	5 yr/M	fourth ventricle	ependymoma	+
48	4 yr/M	fourth ventricle	ependymoma	+ +
49	15 mo/M	lateral ventricle	choroid plexus papilloma	+ + +
50	4 yr/F	lateral ventricle	choroid plexus papilloma	+ +
51	42 yr/F	third ventricle	neuroepithelial (colloidal) cyst	+

Table 4: Non-Neuronal/Glial Tumours of the Nervous System (12 biopsies)

Patient	Age/Sex	Site	Pathological Diagnosis	Cytoplasmic AO-RNA Fluorescence	
52	12 yr/M	pineal	pineal germinoma	+ + + +	(large cells)
				+ +	(small cells)
53	7 yr/F	suprasellar	craniopharyngioma	0	
54	9 yr/M	suprasellar	craniopharyngioma	0	
55	13 yr/M	filum terminale	lipoma	0	
56	7 yr/F	sacral intradural	epidermoid	+	
57	7 yr/F	lumbosacral intradural	dermoid	+ +	
58	3 yr/F	clivus; cerebellopontine angle	chordoma, physaliforous	+ + +	
59	22 yr/F	clivus; posterior fossa subarachnoid	chordoma, physaliforous & chondroidal	+ +	
60	12 yr/M	parietal lobe; leptomeninges	Ewing sarcoma, metastatic	+ +	
61	6 yr/F	cauda equina	Schwannoma	+ +	
62	25 yr/F	ulnar nerve	Schwannoma	+ +	
63	40 yr/F	peroneal nerve	Schwannoma	+ +	

https://doi.org/10.1017/S0317167100035769 Published online by Cambridge University Press

Among primitive neuroblastoma cells, in astrocytoma cells of all degrees of pleomorphism, and in neuroepithelial tumour cells, the orange cytoplasm was more uniform and homogeneous than granular after staining with AO (Figures 3, 9-12). Chordoma cells showed coarse orange granules (Figure 18) which disappeared after ribonuclease digestion and restaining with AO, and correlated well with the extensive rough endoplasmic reticulum shown in the electron micrographs of these cells (Figure 20).

Discussion

The tricyclic acridine orange (AO) molecule combines with nucleic acids to form highly fluorescent complexes. Because the wavelengths of absorption of ultraviolet light and emission of visible light differ, AO-DNA complexes and AO-RNA complexes are perceived in the fluorescence microscope as different colours; DNA appears bright yellow-green while RNA is a luminous orange-red. Tissue proteins and other substances not containing nucleic acids generally appear pale green or nonfluorescent black. An important exception are nonglycogen polysaccharides which fluoresce red when stained with AO, hence the acid mucopolysaccharide granules of mast cells and the cytoplasm of cartilege cells are bright red, potentially causing confusion with RNA. Treatment of the tissue sections by ribonuclease followed by restaining with AO resolves any doubt about the origin of the red fluorescence, since RNA will have been totally digested and the fluorescence abolished. Autofluorescent ceroid-lipofuscin pigment in neurons may be distinguished from DNA by examining unstained sections under ultraviolet light.[4] As with other histochemical stains, the results of AO are relative and qualitative rather than quantitative, but this disadvantage is compensated by the precise cytological localization. AO is considerably more sensitive for cytoplasmic RNA than are the basophilia of hematoxylin stain or the capricious methyl green pyronin method. The physiochemical basis of AO fluorescence was reviewed by Rigler[5] and Kasten.[6]

Figure 19 — Electron micrograph of cell of cerebellar medulloblastoma that was atypical in showing strong AO fluorescence for cytoplasmic RNA (fig 2). Numerous profiles of rough endoplasmic reticulum are seen (arrowheads) although they are not stacked as they are in Nissl substance of mature motor neurons. Abundant free ribosomes also are seen throughout the cytoplasm. Mitochondria (m) appear normal. In other cells of this tumour, microtubular differentiation also was identified. Bar = 1.25 μm

PLATE II (Figs 7-12)

Figure 7 — Patient 22. Pheochromocytoma of adrenal medulla in a 14-year-old boy. The highly differentiated and specialized secretory nerve cells of this tumour show intense orange cytoplasmic fluorescence. AO X250

Figure 8 — Reactive gemistocytic astrocytes near a zone of cerebral infarction show minimal orange AO-RNA fluorescence despite abundant cytoplasm. AO X400

Figure 9 — Patient 26. Low grade astrocytoma of cerebellum in a 7-year-old boy. Cytoplasmic RNA fluoresence of low intensity is demonstrated. AO X100

Figure 10 — Patient 36. Cerebral cortical infiltration by astrocytoma in a 12-year-old boy. The cells containing abundant orange cytoplasm are normal neurons. Astrocytoma cells have only moderate RNA. AO X250

Figure 11 — Patient 43. Malignant astrocytoma in a 3-year-old girl. Considerable pleomorphism is seen, and the cytoplasm of these anaplastic cells shows strong AO-RNA fluorescence. AO X250

Figure 12 — Patient 44. Malignant xanthoastrocytoma in a 15-year-old girl. Strong AO-RNA influence is seen in the cytoplasm of these highly pleomorphic, often multinucleated cells. Immunoperoxidase stain of GFAP demonstrated the astrocytic origin of this neoplasm. AO X250

PLATE III (Figs 13-18)

Figure 13 — Patient 30. Rosenthal fibers in an astrocytoma from a 17-year-old girl show no orange fluorescence, as expected in these degenerating glial processes. AO X100

Figure 14 — Patient 49. Choroid plexus papilloma in lateral ventricle of a 15-month-old boy. The amount of orange cytoplasmic fluorescence in the well differentiated neuroepithelium resembles that of normal choroid plexus. AO X250

Figure 15 — Patient 47. Ependymoma from fourth ventricle of a 5-yearold boy has moderate orange fluorescence of tumour cell cytoplasm, but not of processes forming pseudorosettes with blood vessels. AX X250

Figure 16 — Patient 52. Pineal germinoma in a 12-year-old boy. The large epithelioid cells exhibit strong AO-RNA fluorescence, while the small cells (probably lymphocytes) have much less. AO X400

Figure 17 — Patient 53. Craniopharyngioma in a 7-year-old girl. In this histologically benign tumour not of neuroectodermal origin, no orange RNA fluorescence is detected with AO. X100

Figure 18 — Patient 58. Chordoma cells in a 3½-year-old girl show strong AO-RNA fluorescence, correlating well with the extensive rough endoplasmic reticulum demonstrated by electron microscopy (fig 20) in this case. These cells produce mucinous secretions. AO X400

https://doi.org/10.1017/S0317167100035769 Published online by Cambridge University Press

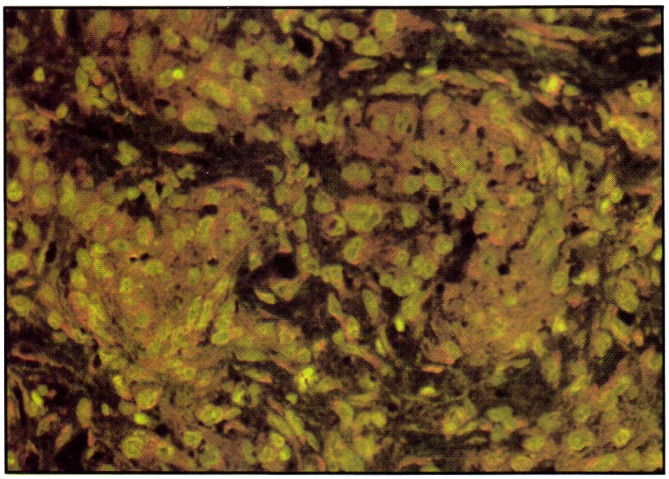

7

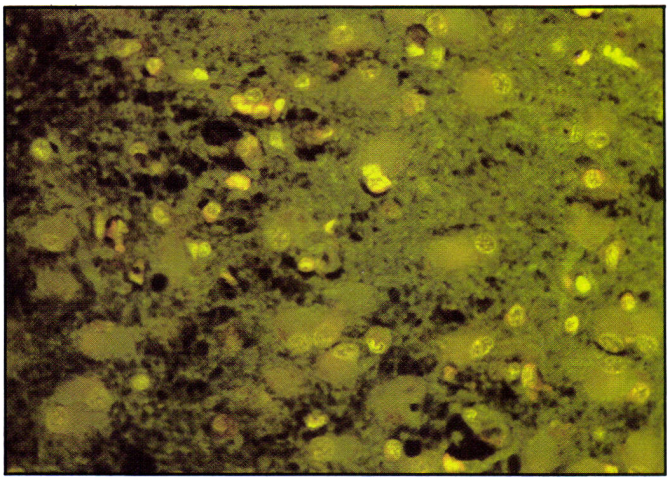

8

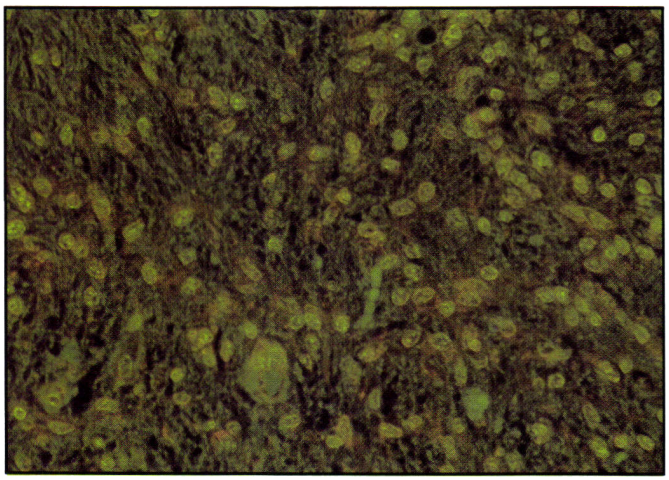

9

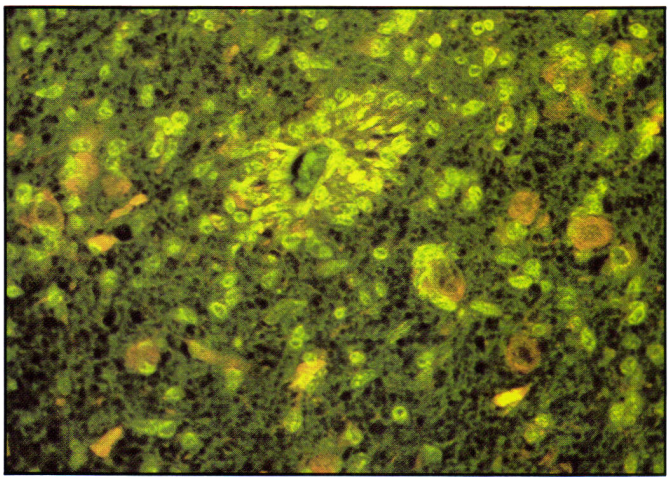

10

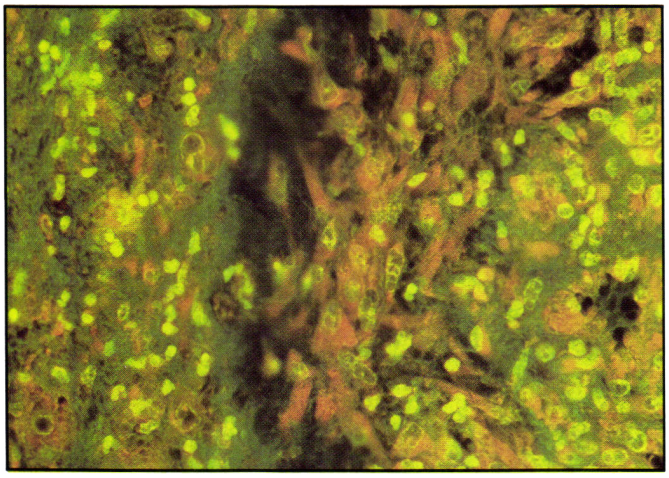

11

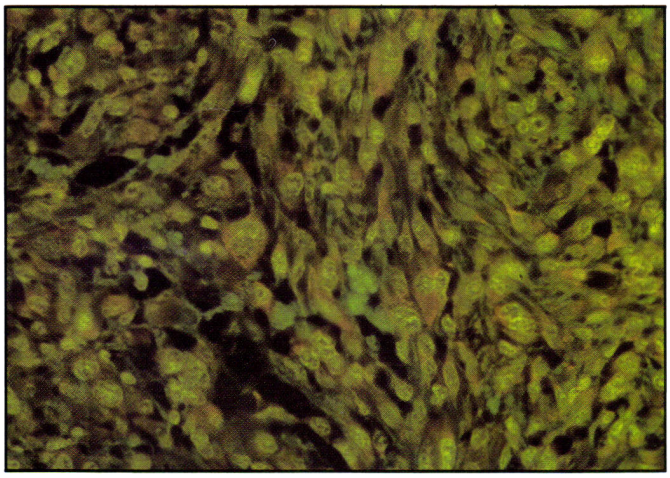

12

https://doi.org/10.1017/S0317167100035769 Published online by Cambridge University Press

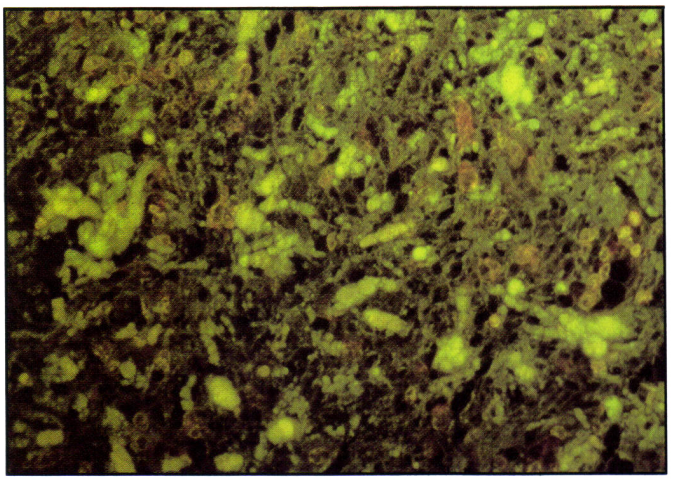

13

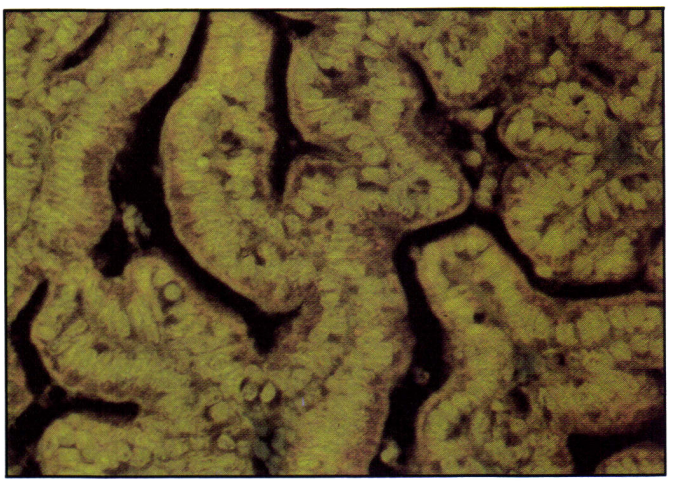

14

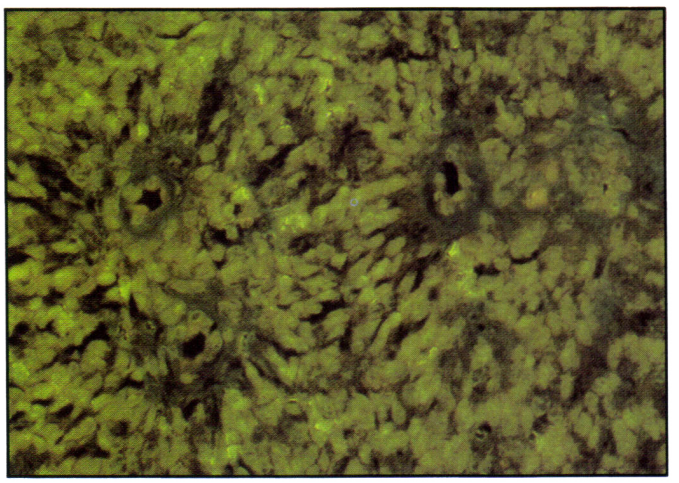

15

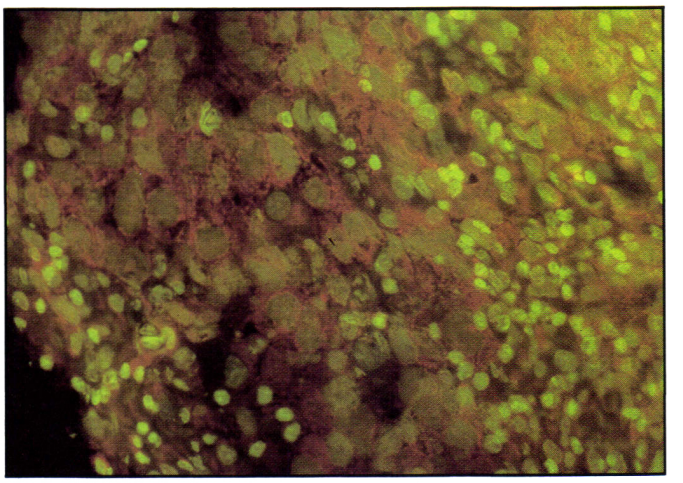

16

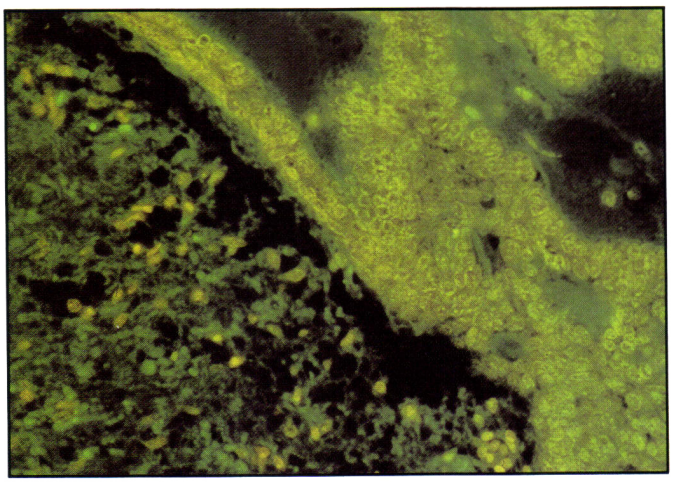

17

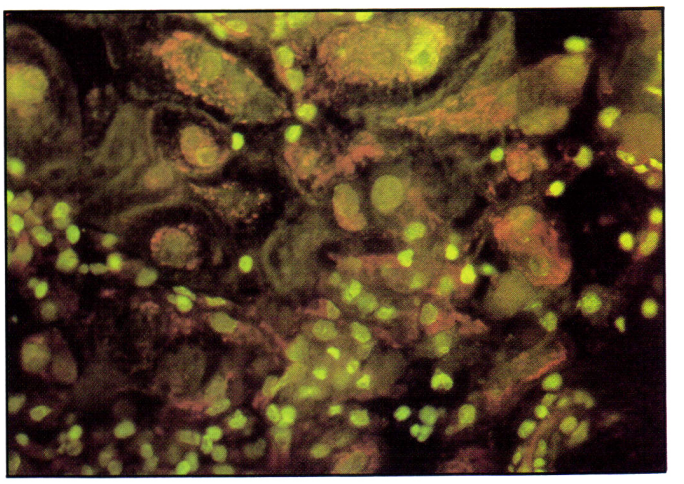

18

https://doi.org/10.1017/S0317167100035769 Published online by Cambridge University Press

The simplicity and rapidity of the AO staining procedure, its adaptability to both unfixed frozen sections and formalin-fixed, paraffin-embedded tissue, and the potential for then restaining the same section with hematoxylin-eosin for ordinary histological examination, all contribute to the practical clinical application of the AO technique. The requirement of an ultraviolet microscope is a minor inconvenience.

Because of the nonquantitative histochemical nature of the AO stain, we do not suggest that it is more precise than present criteria of identifying and grading astrocytomas using standard histological stains and immunoperoxidase antiserum to glial fibrillary acid protein (GFAP). As a special supplementary stain, however, AO has value in recognizing more malignant cells within predominantly low grade astrocytomas, and may be particularly useful in helping distinguish reactive gliosis from well differentiated glioma. Astrocytes including gemistocytes (Figure 8) have less demonstrable cytoplasmic RNA than even the most highly differentiated astrocytoma cells. The relatively high content of RNA in normal choroid plexus epithelium and in the histologically identical choroid plexus papilloma shown by AO probably is related more to the specialized secretory function of these cells than to their rate of protein synthesis or their maturity.

The amount of AO-RNA fluorescence demonstrated in the various tumours in this study correlates with ultrastructural and biochemical data regarding ribosomes in normal and neoplastic cells of the nervous system.[7-10] Normal astrocytes and well differentiated astrocytoma cells have few organelles and only sparse rough endoplasmic reticulum or free cytoplasmic ribosomes demonstrated by electron microscopy; normal oligodendrocytes have more ribosomes than do astrocytes.[7,8] The pleomorphic cells of malignant astrocytomas and glioblastoma mutiforme, by contrast, have much more organelle structures and more numerous ribosomes, both free and membrane-associated.[8,10] Astrocytic RNA is mainly nuclear (i.e. nucleolar) while neuronal RNA is almost all cytoplasmic.[11] The extraordinary RNA content of mature neurons provides a brilliant metachromatic contrast with the background neuropil when stained by AO and examined under ultraviolet light.[2] However, immature neurons such as those found in the periventricular germinal matrix of premature infants show little RNA by either ultrastructural or biochemical examination.[12] As expected, these nerve cells show very weak AO-RNA fluorescence in their cytoplasm during developmental or migratory stages, until after they have reached their final destinations in the brain and begin the processes of synaptogenesis and neurotransmitter biosynthesis.[13]

Marked differences are found between neuronal and glial-enriched fractions of cerebral cortex in the kinetics of incorporation of ^{14}C-labelled orotic acid into RNA; the in vitro synthesis of RNA is initially slower in neurons but its specific activity then increases to levels two to threefold higher between 3 and 6 hours.[11] Another study using [^{3}H] cytidine or [^{3}H] orotic acid showed much greater incorporation of both precursors into neuronal than into glial fractions at all times.[14]

A potential application of AO is in the evaluation of chemotherapy or radiotherapy, upon examining recurrent tumour tissue surgically resected or at autopsy. Such medical treatment, if effective, might be expected to decrease the rate of synthesis of transfer or messenger RNA in neoplastic cells. This effect could be qualitatively measured using AO as a histochemical stain. Ribonuclease activity in human cerebrospinal fluid (CSF) is elevated in patients with brain tumours, even in the presence of normal CSF protein and the absence of red or white blood cells.[15] The significance of this finding is uncertain, but correlation with AO-demonstrated RNA in tumour tissue from such patients may explain the phenomenon and lead to a more specific preoperative CSF test of tumour type.

The cerebellar medulloblastoma is now generally reclassified simply as a primitive neuroectodermal round cell tumour, some being undifferentiated and others showing variable differentiation of glial, ependymal, or neuronal components.[16] Such multipotential differentiation of medulloblastoma is further supported by the demonstration of GFAP in some of these tumours.[17] Similar multipotential maturation also is found by immunocytochemical studies of subependymal giant cells in fetal tuberous sclerosis.[18] Even normal neuroectodermal cells of the subependymal germinal matrix in late fetal life and early infancy still exhibit some mitotic activity associated with both multipotential normal differentiation and potential neoplasia.[19,20] The great majority of these germinal matrix cells become normal neurons.

The variable differentiation of neuroectodermal tumours is based in part on special histochemical and immunocytochemical stains. Our findings with AO in these tumours suggest that this stain may provide one additional criterion in their classification and in understanding their biological behaviour. Normal germinal matrix cells have minimal cytoplasmic RNA and exhibit

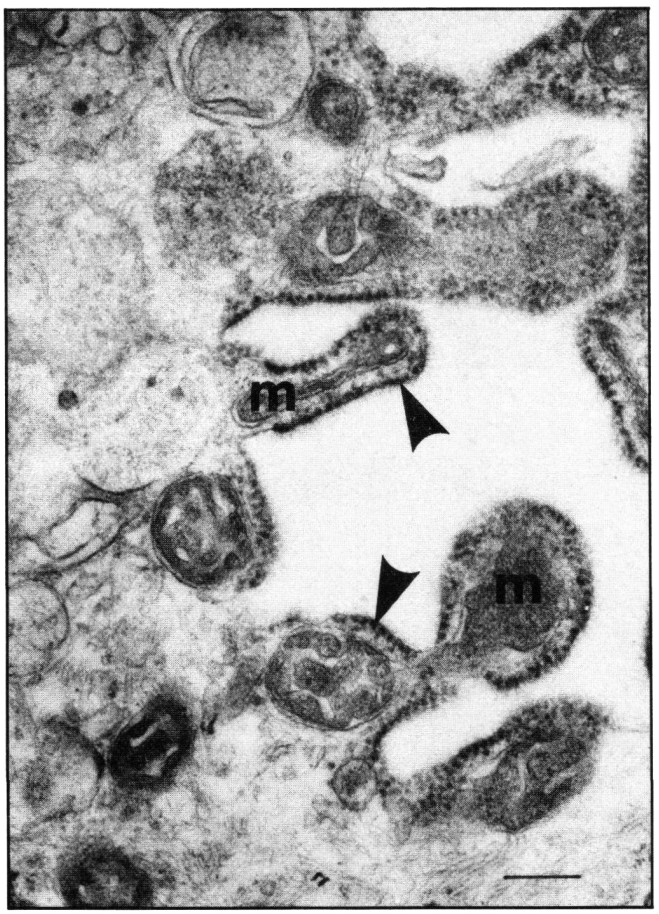

Figure 20 — Ultrastructure of chordoma cell confirms the presence of abundant cytoplasmic RNA shown by AO fluorescence (fig 18). Rows of membrane-associated ribosomes (arrowheads) surround mitochondria (m) in a characteristic fashion. Bar = 0.25 μm

https://doi.org/10.1017/S0317167100035769 Published online by Cambridge University Press

no demonstrable AO-RNA fluorescence.[13] Of the 9 histologically characteristic medulloblastomasof the cerebellum examined in this study, all except one plus our single case of retinoblastoma showed no or minimal cytoplasmic RNA fluorescence. The remaining histologically typical medulloblastoma (Case 10) suprisingly showed strong orange cytoplasmic fluorescence (Figure 2); this high RNA content was confirmed by electron microscopy (Figure 19). The 3 cerebral tumours diagnosed histologically and immunocytochemically as primitive neuroectodermal tumours also showed strong fluorescence for RNA. These findings suggest not only that there may be fundamental difference between primitive neuroectodermal tumours of cerebral and of cerebellar origin, but that those in the latter site, the medulloblastomas, also may be separated into two groups based on low or high RNA production. In a sense, those with high concentration of cytoplasmic RNA still follow the gradient of the neuronal series because of more rough endoplasmic reticulum, microtubules, and other subcellular structures characteristic of neurons. These features suggest that neuroectodermal tumour cells with strong AO-RNA fluorescence are differentiating as neurons, while medulloblastoma and retinoblastoma cells with sparse RNA remain undifferentiated.

The opposite gradients of the neuronal and of the neuroglial series of tumours is incompletely understood. While high concentrations of cytoplasmic RNA are explicable in functionally secretory tumours such as pheochromocytoma and choroid plexus papilloma, as well as in maturing neurons of ganglioneuromas and gangliogliomas, the reason for these high RNA concentrations is not as evident in the poorly differentiated cells of the astrocytic series, as in malignant astrocytomas. The anaplastic cells of glioblastoma multiform in the adult show a similar strong orange cytoplasmic fluorescence with AO unrelated to the nuclear/cytoplasmic ratio or to mitotic activity (our own unpublished observations). Chromosomal aberrations in number or morphology among such neoplastic cells might be one correlate.

More study is needed to determine whether a gradient might also exist among reactive astrocytes in terms of age of the lesion, similar to that shown in neoplastic cells of the central nervous system. The four cases of gemistocytic astrocytosis in our present series were all chronic, but acute reactive glial cells might exhibit more RNA. We are presently studying this problem.

Finally, many unresolved questions are not addressed by this study. What type of RNA is present in tumour cells: transfer RNA, messenger RNA or another type? Is there a correlation of RNA content of tumour cells with biological behaviour of the neoplasm and clinical course? Do medulloblastomas with abundant RNA have better of worse prognosis than those with sparse RNA? Do chemotherapy and radiotherapy affect RNA production in tumour cells? The acridine orange technique together with quantitative biochemical methods for studying nucleic acids, may offer a means by which such questions can be answered.

Acknowledgement

We wish to thank the many physicians and surgeons who provided clinical care of the patients in this study and who submitted tissue for examination. We particularly acknowledge Drs. D.D. Cochrane, H.Z. Darwish, R.H.A. Haslam, S.T. Myles, S.Z. Rubin, and C.G.F. Seagram for their contributions. Drs. A. Clark, H.Z. Darwish, and R.H.A. Haslam offered helpful suggestions in preparing this paper. Ms. Y. Smink, L. Hines, P. Steward, A. Elash, and F. Jahelka provided technical laboratory assistance. Ms. B. Cooper typed the manuscript. This study was supported by a grant to Dr. H.B. Sarnat from the Alberta Children's Hospital Foundation.

References

1. Perl DP, Little BW. Acridine orange-nucleic acid fluorescence. Its use in routine diagnostic muscle biopsies. Arch Neurol 1980; 37: 641-644.
2. Sarnat HB. L'acridine-orange: un fluorchrome des acides nucléiques pour l'étude des cellules musculaires et nerveuses. Rev Neurol (Paris) 1985; 141: 120-127.
3. Sarnat HB, Seagram CGF, Trevenen CL, Rubin SZ. A fluorochrome stain for nucleic acids to demonstrate submucosal and myenteric neurons in Hirschsprung's disease. Am J Clin Pathol 1985; 83: 722-725.
4. Sarnat HB. Occurrence of fluorescent granules in the Purkinje cells of the cerebellum. Anat Rec 1968: 162: 25-32.
5. Rigler R Jr. Microfluorometric characterization of intracellular nucleic acids and nucleoproteins by acridine orange. Acta Physiol Scand 1966; 67: suppl 267.
5. Kasten FH. Cytochemical studies with acridine orange and the influence of dye contaminants in the staining of nucleic acids. Int Rev Cytol 1967; 21: 141-202.
7. Peters A, Palay SL, Webster H de F. The fine structure of the nervous system: The neurons and supporting cells. Philadelphia: WB Saunders. 1976.
8. Duffy PE. Astrocytes: Normal, reactive, and neoplastic. New York: Raven Press 1983; 43.
9. Poon TP, Hirano A, Zimmerman HM. Electron microscopic atlas of brain tumors. New York: Grune and Stratton. 1971.
10. Dolman CL. Ultrastructure of Brain Tumors and Biopsies. A diagnostic atlas. NY: Praeger Publishers. 1984; 1-60.
11. Volpe P, Guiditta A. Biosynthesis of RNA in neuron-glia-enriched fractions. Brain Res 1967; 6: 228-240.
12. Lindholm DB, Khawaja JA. Distribution and protein synthetic activities of neuronal free and membrane-bound ribosomes during postnatal development of rat cerebral cortex. Neuroscience 1983; 9: 645-651.
13. Sarnat HB. Étude fluorochromique d'ARN de neurons en développement normal et dans la dysgénésie cérébrale. Can J Neurol Sci 1985; 12: 185 (abstract).
14. Flangas AL, Bowman RE. Differential metabolism of RNA in neuronal-enriched and glial-enriched fractions of rat cerebrum. J Neurochem 1970; 17: 1237-1245.
15. Rabin EZ, Weinberger V, Tattrie B. Ribonuclease activity of human cerebrospinal fluid. Can J Neurol Sci 1977; 4: 125-130.
16. Rorke LB. The cerebellar medulloblastoma and its relationship to primitive neuroectodermal tumors. J Neuropathol Exp Neurol 1983; 42: 1-15.
17. Kumanishi T, Washiyama K, Watabe K, Sekiguchik K. Glial fibrillary acidic protein in medulloblastomas. Acta Neuropathol 1985; 67: 1-5.
18. Nishimura M, Takashima S, Takeshita K, Tanaka J. Immunocytochemical studies on a fetal brain of tuberous sclerosis. Pediat Neurol 1985; 1: 245-248.
19. Vick NA, Lin M-J, Bigner D. The role of the subependymal plate in glial tumorigenesis. Acta Neuropathol 1977; 40: 63-71.
20. Rakic P. Neuronal-glial interaction during brain development. Trends in Neurosciences 1981; 4: 184-187.